

# Measurements of r-process nuclei

K.-L. Kratz<sup>a</sup>

<sup>a</sup>Institut für Kernchemie, Universität Mainz, D-55128 Mainz, Germany

Progress in the astrophysical understanding of r-process nucleosynthesis also depends on the knowledge of nuclear-physics quantities of extremely neutron-rich isotopes. In this context, experiments at CERN-ISOLDE have played a pioneering role in exploring new shell-structure far from stability. Possible implications of new nuclear-data input on the reproduction of r-abundance observations are presented.

## 1. General motivation

Relative to other fields, explosive nucleosynthesis is probably unique in its requirements of a very large number of (nuclear-) physics quantities in order to achieve a satisfactory description of the astrophysical phenomena under study. Because nuclei of extreme  $N/Z$  composition exist in explosive environments, an understanding of their nuclear-structure properties has always been and still is a stimulating challenge to the experimental and theoretical cosmo-chemistry and nuclear-physics community.

## 2. R-abundance peaks and neutron shell-closures

About 40 years ago, Charles D. Coryell, in his important but widely unrecognized article on *"The Chemistry of Creation of the Heaviest Elements"* [1], has summarized his ideas about the importance of shell-structure from the 1950's for the formation of elements of mass number  $A > 70$  by rapid neutron capture. Starting with the realization, that historically *"chemists have been interested from time immemorial in the chemical composition of the world around us"*, he emphasizes the importance of the neutron shell-closures at  $N=50, 82$  and  $126$  for the time-scale of the fast neutron-capture process and the *"r-process pile-up"* at the bromine, xenon and platinum peaks of Suess and Urey's so-called *"cosmic abundances"* [2]. As *"primary antecedent (odd-Z) species with  $N=50$ "*, already at that time Coryell favours  $^{79}\text{Cu}$  and  $^{81}\text{Ga}$ . He considers these isotopes out of experimental reach, because they are *"even more neutron-rich than primary fission products"*. On the basis of their isobaric *"displacement from the valley of stability"*, he estimates a half-life of about 0.1 s. Similarly, for  $N=82$ , Coryell suggests that the decay of the precursors  $^{127}\text{Rh}$ ,  $^{129}\text{Ag}$  and  $^{131}\text{In}$  forms the top of the  $A \simeq 130$  abundance peak; and for  $A \simeq 195$  peak *"topped by  $^{195}\text{Pt}$ "* he assigns  $^{195}\text{Tm}$  as the primary  $N=126$  nucleus. With his further assumption *"that the energy of first decay, and thus the probable half-life for the decay, stays about constant"* along the r-process path, the total time required for a steady-state build-up of heavy nuclides from Fe to U would be roughly 6.5 s. It is

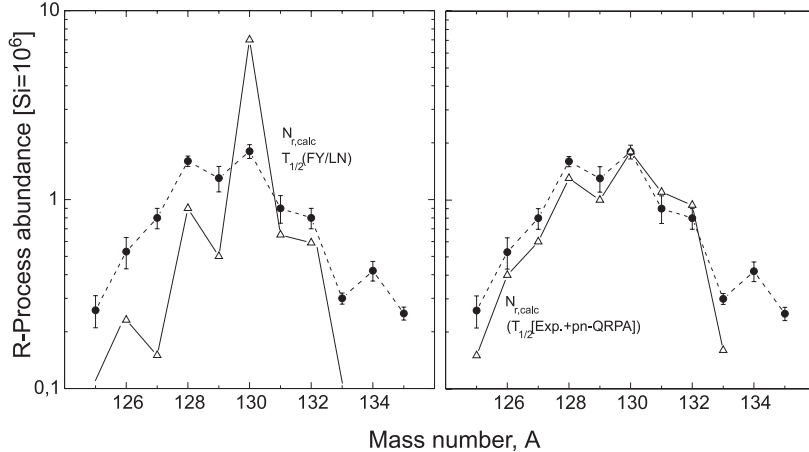


Figure 1. Static calculations of  $A \approx 130$  r-abundances assuming  $S_n = \text{const}$  and  $N_{r,\odot}(Z) \times \lambda_{\beta}(Z) = \text{const}$ . In the left part, theoretical  $T_{1/2}$  and  $P_n$  values from straight-forward QRPA calculations [8] neglecting effects from the p-n residual interaction are depicted. The right part shows an improved fit with the same  $\beta$ -flow assumptions, but now using measured  $\beta$ -decay data and QRPA predictions fine-tuned to reproduce nuclear-structure properties around  $^{132}\text{Sn}$  known in the early 1990's. In both cases, masses from an early version of the 1995 FRDM [9] were used in the calculations of the gross  $\beta$ -decay properties.

interesting to compare this estimate with the contemporary one of Burbidge et al. [3] of about 80 s.

Today, we know that the r-process matter flow is not constant. It is fast in the mass regions between the magic neutron numbers, whereas the shell-closures act as "bottle-necks". Here, at  $N=50, 82$  and  $126$ , each, the classical r-process needs several hundred milliseconds to pass these regions, thereby building up the well known r-abundance peaks observed in the solar system ( $N_{r,\odot}$ ). Therefore, the nuclear-physics input to these  $N_{r,\odot}$  maxima is still today of particular importance for the understanding of r-process nucleosynthesis, independent of its stellar site.

Still some 15 years ago, astrophysicists believed that nuclear-structure information on r-process nuclei, lying 14 ( $_{28}\text{Ni}$ ) to 36 ( $_{63}\text{Eu}$ ) mass units away from the  $\beta$ -stability line, would never be accessible to experiments on earth. However, continued progress in ion-source and mass-separator technology has soon after resulted in the identification of the first two classical, neutron-magic "waiting-point" isotopes [3],  $^{80}\text{Zn}_{50}$  and  $^{130}\text{Cd}_{82}$  at OSIRIS, TRISTAN and ISOLDE, respectively [4–6]. As was shown in [6,7], with their  $\beta$ -decay properties first evidence for the existence of the earlier postulated  $N_{r,\odot}(Z) \times \lambda_{\beta}(Z) \approx \text{const}$ . correlation could be achieved. We would, however, remind the r-process laymen that this is a rather crude correlation based on simple **static** calculations with the assumption of constant neutron-separation energies ( $S_n$ ) for all ( $N_{\text{mag}}+1$ ) nuclei at the "staircases" associated with the rising sides of the  $N_{r,\odot}$  peaks (see, e.g., Fig. V,3 in [3], or Figs. 9 and 10 in [7]). In this approach, exclusively the  $\beta$ -decay rate ( $\lambda_{\beta}$ ) or the half-life ( $T_{1/2} = \ln 2 / \lambda_{\beta}$ )

of the neutron-magic nuclides are of importance. Nevertheless, at those times when the predictions for the  $T_{1/2}$  of  $N=82$   $^{130}\text{Cd}$ , for example, varied between 30 ms and 1.2 s, our experimental value of  $T_{1/2}=(196\pm 35)$  ms was of considerable importance to constrain the equilibrium conditions of an r-process within the above approximation. The result of such calculations of the  $A\simeq 130$   $N_{r,\odot}$  peak some 10–15 years ago is depicted in Fig. 1. In the left part, straightforward  $T_{1/2}$  calculations are shown using the Quasi-Particle Random-Phase Approximation (QRPA) of Ref. [8] with Folded-Yukawa wave functions, a Lipkin-Nogami pairing model and the (presumably too low) masses from an early version of the 1995 Finite-Range Droplet Model (FRDM) [9], but neglecting proton-neutron (p-n) residual interaction. For comparison, in the right part of this figure, our again static r-abundance calculations from the early 1990's with experimental data on  $^{131,133}\text{In}$  and  $^{130}\text{Cd}$  and an improved QRPA version, now taking into account effects of the p-n interaction are depicted (see, e.g. Ref. [10]). Nowadays, with our largely improved knowledge on nuclear masses and  $\beta$ -decay properties of nuclei far from stability as input for time-dependent "canonical" or dynamical r-process network calculations (see, e.g., [11–14]), the above simplistic static picture should therefore no longer be used for abundance simulations.

In any case, the experimental success in the late 1980's strongly motivated further experimental and theoretical nuclear-structure investigations and its possible astrophysical implications. For example, the second  $N=50$  waiting-point isotope  $^{79}\text{Cu}$  could be identified [15]. Furthermore, the measured high delayed-neutron emission probabilities ( $P_n$ ) of odd- $Z$  r-process nuclei just beyond  $N=50$  were shown to be the nuclear-structure origin of the odd-even staggering in the  $N_{r,\odot}$  peak at  $A\simeq 80$  [16]; and from the interpretation of the  $^{80}\text{Zn}_{50}$  decay scheme, first evidence for a vanishing of the spherical  $N=50$  shell closure far from stability was obtained [17].

Since the late 1980's, important progress has been achieved in the understanding of the systematics and development of nuclear-structure with increasing neutron excess (see, e.g. [18–20]), with CERN-ISOLDE always playing a leading role in this field. However, due to the generally very low production yields, the restriction to chemically non-selective ionization modes, or the application of non-selective detection methods, no further information on isotopes lying **on** the r-process path could be obtained for quite some time. Only in recent years, the identification of additional r-process nuclides has become possible thanks to considerable improvements of the **selectivity** in production and detection methods of rare isotopes, e.g. by applying resonance-ionisation laser ion-source (RILIS) systems.

### 3. Recent experiments

Today, there are mainly three mass regions, where nuclear-structure properties of specific interest to r-process nucleosynthesis can be studied experimentally. The first is the classical r-process seed region involving very neutron-rich Fe-group isotopes in the vicinity of the doubly-(semi-)magic nuclei  $^{68}\text{Ni}_{40}$  and  $^{78}\text{Ni}_{50}$ . Recent spectroscopic results can, for example, be found in [21,22]. The second region is that of far-unstable nuclei around  $A\simeq 115$ . Here, most canonical r-process calculations show a pronounced r-abundance trough, which we believe to be due to nuclear-model deficiencies in predicting ground-state shapes and masses at and beyond  $N=72$  mid-shell (see, e.g. [11,23]). Recent experimental information on that mass range can be found, e.g. in [21,22,24,25].

The third region of interest, on which the main focus of this paper has been put, is that around the doubly-magic nucleus  $^{132}_{50}\text{Sn}_{82}$ . Apart from its astrophysical importance (*the r-process matter flow through the  $A \simeq 130$   $N_{r,\odot}$  peak*) [11,13], this area is of considerable shell-structure interest. The isotope  $^{132}\text{Sn}$  itself, together with the properties of the nearest-neighbour single-particle ( $^{133}_{51}\text{Sb}_{82}$  and  $^{133}_{50}\text{Sn}_{83}$ ) and single-hole ( $^{131}_{50}\text{Sn}_{81}$  and  $^{131}_{49}\text{In}_{82}$ ) nuclides are essential for tests of the shell model, and as input for future nuclear-structure calculations towards the neutron-drip line.

The bulk of data so far known in this mass region have been obtained from  $\beta$ -decay spectroscopy at the mass-separator facilities OSIRIS and ISOLDE [19–22,24,25]. During the past few years, new data "northeast" of  $^{132}\text{Sn}$  were published also from spontaneous-fission studies of  $^{248}\text{Cm}$  (see, e.g., Korgul et al. [26], and Refs. therein). With respect to the closest neighbours of  $^{132}\text{Sn}$ , the structures of  $^{131}\text{Sn}_{81}$  ( $\nu$ -hole) and  $^{133}_{51}\text{Sb}$  ( $\pi$ -particle) are fairly well known since more than a decade. More recently, the lowest  $\nu$ -particle states in  $^{133}\text{Sn}_{83}$  have been identified at the General Purpose Separator (GPS) of the PS-Booster ISOLDE facility (see, e.g., Hoff et al. [27]). From these data, valuable information on the spin-orbit splitting of the 2f- and the 3p-orbitals was obtained. These results were compared to mean-field and HFB predictions, and it was found that none of the potentials used in the past in *ab initio* shell-structure calculations was capable of properly reproducing the ordering and spacing of these states.

With these new data, the close  $^{132}\text{Sn}$  valence-nucleon region is nearly complete. The only missing information are the  $\pi$ -hole states in  $^{131}_{49}\text{In}$ , which can in principle be studied through  $\beta$ -decay of the exotic nucleus  $^{131}\text{Cd}_{83}$ . Off-line test experiments to find a well-suited excitation scheme for resonance ionization of Cd were initially carried out in Mainz [28]; and first results on  $T_{1/2}$  data and delayed-neutron emission probabilities ( $P_n$ ) of  $N=82$  to  $84$   $^{130-132}\text{Cd}$  using a similar laser system were obtained at ISOLDE. A detailed discussion of the initially quite surprising results for  $N=83$   $^{131}\text{Cd}$  and  $N=84$   $^{132}\text{Cd}$  can be found in Ref. [29]. Already these gross properties indicate again that the structure below and beyond  $^{132}\text{Sn}$  is not at all well understood by now. Of direct astrophysical importance is our new measurement of the  $N=82$  waiting-point nucleus  $^{130}\text{Cd}$ . Its considerably improved half-life of  $T_{1/2}=(167\pm 7)$  ms is somewhat lower than our old value from 1986 of  $(195\pm 35)$  ms [6], but still lies within the error limits given at that time. The measured  $P_n$  value of  $(3.5\pm 1.0)$  % is in agreement with our earlier estimate.

Another important observation with respect to the calculation of  $\beta$ -decay properties of so far unknown  $N \simeq 82$  r-process waiting-point isotopes is that model predictions of  $Q_\beta$  values in the region "south" of  $^{132}\text{Sn}$  differ considerably, with the general tendency that those models which exhibit a strong  $N=82$  shell closure (e.g., FRDM [9] or ETFSI-1 [30]), give the "lower" values. Recent increasing experimental evidence of a weakening of the classical shell-structure below  $^{132}\text{Sn}$  (see, e.g. [21,22,29,31,32]), however, seem to favour the systematically higher  $Q_\beta$  predictions from mass models with "shell-quenching" (e.g., HFB/SkP[33] or ETFSI-Q[34]) below  $^{132}\text{Sn}$ . This trend is of particular importance for the  $T_{1/2}$  and  $P_n$  predictions of  $Z < 50$ ,  $N=82$  r-process waiting-point nuclei. Sizeable differences in the  $Q_\beta$  values between un-quenched and quenched mass models start at  $^{131}\text{In}$  with  $\Delta Q_\beta \simeq 400$  keV, continue via  $^{130}\text{Cd}$  to  $^{127}\text{Rh}$  with about 1 MeV, and range down to  $^{122}\text{Zr}$  with  $\Delta Q_\beta \simeq 4$  MeV, resulting in considerable changes in theoretical  $T_{1/2}$  for these isotopes. For  $^{130}\text{Cd}$ , for example, the  $T_{1/2}(\text{QRPA})$  with  $Q_\beta(\text{ETFSI-Q})=8.30$  MeV is a

factor 2.5 shorter than with  $Q_\beta(\text{FRDM})=7.43$  MeV. It is interesting to note in this context that the same trend is completely independently predicted also by very recent shell-model calculations of B.A. Brown et al. [35]. Therefore, in order to solve the above discrepancies, high-precision mass measurements in the region below  $^{132}\text{Sn}$  are foreseen at ISOLDE using the Penning-trap mass spectrometer ISOLTRAP. In any case, in our more recent r-process calculations, we prefer to use newly calculated  $T_{1/2}(\text{GT+ff})$  values, which supercede our 1996 evaluation [36] applied in earlier r-process studies. It should be pointed out in this context, that already since the early 1990's our astrophysics collaboration uses steadily updated evaluations of experimental and theoretical  $T_{1/2}$  and  $P_n$  values, in which the calculated gross properties are based on the FRDM mass and deformation parameters [9] and contain a microscopic GT-strength [8] and a schematic ff-strength [37]. For neutron-rich  $A \simeq 130$  isotopes, this led already in the past to shorter  $T_{1/2}$  and smaller  $P_n$  values than listed in [38]. Therefore, we would appreciate if the rather general statement in a number of recent papers that some new shell-model half-lives are significantly shorter than those "*currently adopted in r-process simulations*" could be put more precisely in the future. At least, as far as our Basel–Los Alamos–Mainz collaboration is concerned, our theoretical  $T_{1/2}(\text{GT+ff})$  are quite similar to the new shell-model values. Hence, statements that those new values would speed up the r-matter flow in the neutron-magic bottle-neck regions do not concern our calculations.

Another recent study of nuclear-structure developments towards  $N=82$  is related to the  $\beta\text{dn-}$  and  $\gamma$ -spectroscopic measurements of neutron-rich Ag nuclides at CERN-ISOLDE, again using an optimized RILIS system for this element. This Z-selectivity was of considerable assistance in minimizing the activities from unavoidable surface-ionized In and Cs isobars. In this context, the additional selectivity of the spin- and moment-dependent hyperfine (HF) splitting was used to enhance the ionization of either the  $\pi p_{1/2}$  isomer or the  $\pi g_{9/2}$  ground-state (g.s.) decay of the Ag isotopes. Details about first  $\beta\text{dn-}$  and  $\gamma$ -spectroscopic applications of this technique to short-lived isomers of  $^{122}\text{Ag}$  up to the classical  $N=82$  r-process waiting-point nuclide  $^{129}\text{Ag}$  can be found, e.g. in [24,21,22]. Because of its importance for r-process calculations, in particular for the time spent in the  $A \simeq 130$   $N_{r,\odot}$  peak region, some details about the difficulties in the measurement of this latter isotope are given. Only after fine-tuning the lasers to an off-center frequency leading to an enhancement of the ionization of the  $\pi g_{9/2}$  level relative to the  $\pi p_{1/2}$  state, an unambiguous identification of the g.s.  $\beta\text{dn-}$ decay of  $^{129}\text{Ag}$  with a  $T_{1/2}=(46_{-9}^{+5})$  ms was possible (see, e.g. Fig. 10 in [22]). The measured  $T_{1/2}(\text{g.s.})$  value is longer than our initial QRPA(Nilsson/BCS) estimate of 15 ms, but is in good agreement with our more recent QRPA(FY/LN) prediction [38] and two subsequent shell-model calculations of Refs. [39,35]. However, the measured  $T_{1/2}(\text{g.s.})$  is lower than our old static waiting-point *requirement* of about 130 ms [7,11]. Within this simple approach, the 46 ms would not be enough to build-up the  $^{129}\text{Xe}$  r-abundance to its solar value (see the left part of Fig. 1 in this context), but – as we will see later (in Figs. 2,3) – for more realistic dynamic calculations with (non-constant)  $S_n$  values, e.g. from the ETFSI-Q mass model, the measured  $T_{1/2}(\text{g.s.})$  for  $^{129}\text{Ag}$  fits much better. Furthermore, when requiring a really "perfect" fit at  $A=129$  one will have to consider also smaller effects from non-equilibrium phases of the r-process, e.g. neutron capture and neutrino processing during freeze-out. Under such conditions, also the  $T_{1/2}$  contribution from the  $\pi p_{1/2}$  isomer might be of importance

for the residual "stellar" half-life of  $^{129}\text{Ag}$ . We calculate a value of  $T_{1/2}(\text{GT}+\text{ff})\simeq 125$  ms for this isomer, in reasonable agreement with the very recent shell-model prediction of 89 ms by B.A. Brown. As is discussed e.g. in [40], with an isomeric half-life in this range, a stellar  $T_{1/2}\simeq 60\text{--}72$  ms would result after neutron capture on  $^{128}\text{Ag}$  to form an excited  $^{129}\text{Ag}$  nucleus, which then  $\gamma$ -cascades down to the isomer and the g.s. And, indeed, a careful comparison of the  $A=129$   $\beta$ dn-decay curves taken under "laser-off" and "laser-on" conditions at central frequency, gave a first indication of a weak, longer-lived  $^{129}\text{Ag}$  component with a  $T_{1/2}$  in the range 80–160 ms. Now, it will be important to use isomer-specific ionization in combination with isobar separation at the High-Resolution Separator (HRS) of ISOLDE to ascertain the existence of this  $\pi p_{1/2}$  isomer with a half-life different from the g.s.-decay.

Because of space limitations, our  $\gamma$ -spectroscopic data on the decay of heavy Ag isotopes, in particular the extension of the  $2^+$  and  $4^+$  level systematics up to  $^{128}\text{Cd}$  and tentatively to  $N=82$   $^{130}\text{Cd}$ , cannot be discussed here. Therefore, we only mention that our data indicate a weakening of the spherical  $N=82$  shell below doubly-magic  $^{132}\text{Sn}$ , as predicted by some theories. For details, we refer to our recent publications [22,32]. Finally, also our very recent first experiment on the decays of very neutron-rich Sn isotopes, again using RILIS at ISOLDE, should be mentioned [41]. The data are not yet fully analyzed, but already now the new  $\beta$ -decay properties of  $^{135\text{--}137}\text{Sn}$  indicate that they may help to improve our r-abundance fits in the  $A=134$  to  $A=140$  mass region (see Figs. 2,3).

#### 4. Fitting the $A\sim 130$ $N_{r,\odot}$ peak region

In particular since the recent astronomical observations of the possible existence of (at least) two r-process components from different sites, a **primary main** r-process responsible for the heavy elements between Cd and the Th–U region [42], and a **secondary weak** r-process requested to produce the lighter elements in and beyond the  $A\sim 80$  peak [43,44], the  $N=82$ ,  $A\sim 130$  waiting-point region has gained additional importance as the *first* bottle-neck in the main-component r-matter flow. Now – without the  $N=50$ ,  $A\sim 80$  peak – the Xe–Te peak determines to a considerable extent the total time needed for this process in the (still favourably discussed) SN II scenario (see, e.g. [45,46,14]). Based on our new experimental  $T_{1/2}$  and  $P_n$  values for  $^{130}\text{Cd}$  and  $^{129}\text{Ag}$ , together with the considerably improved understanding of the nuclear-structure properties in the  $^{132}\text{Sn}$  region which have been incorporated into our recent QRPA calculations for the so far unknown ( $Z<47$ )  $N=82$  waiting-point isotopes, a quite satisfactory reproduction of the total r-abundance curve can be obtained in time-dependent, multi-component "canonical" r-process calculations (see, e.g. [40,22,14]).

Since we want to focus here on the  $N=82$  waiting-point region, we present in Figs. 2,3, a cut-out in linear scale of our latest  $\beta$ -flow r-abundance calculations. They are plotted together with the latest  $N_{r,\odot}$  "residuals" from the compilation of Arlandini et al. [47]. From a comparison of these figures, one can draw several conclusions which may clarify the situation about the build-up of the  $A\sim 130$   $N_{r,\odot}$  peak and the time needed to overcome this bottle-neck towards heavier r-isotopes. In Fig. 2, we first show two "fits" with the initial simplistic assumption of constant  $S_n=2$  MeV values for all  $N=83$  isotopes between  $_{40}\text{Zr}$  and  $_{49}\text{In}$ , in one case "normalized" to the top of the  $N_{r,\odot}$  peak at  $A=130$  (left part, where

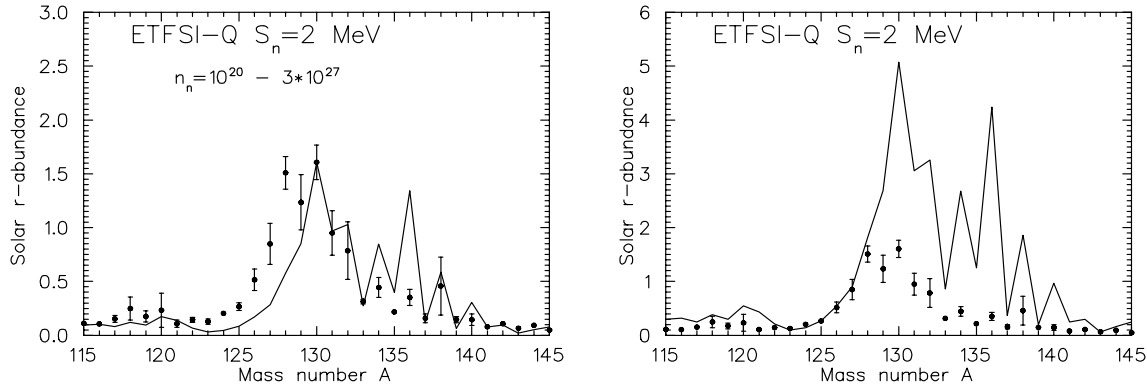


Figure 2. R-abundances in the  $A \simeq 130$  region from dynamical calculations with the simplistic assumption of  $S_n = \text{const}$  for all  $N=83$  isotones between  ${}_{40}\text{Zr}$  and  ${}_{49}\text{In}$ , in the left part "normalized" to the top of the  $N_{r,\odot}$  peak at  $A=130$ , and – alternatively – in the right part to the bottom of the rising part of the peak at  $A=125$ .

$N=82$   ${}^{130}\text{Cd}$  is the main progenitor) and in the other case to the bottom of the left wing of the peak at  $A=125$  (right part, where  $N=82$   ${}^{125}\text{Tc}$  is the main progenitor). One can easily imagine that both presentations may give rise to completely misleading interpretations. The assumption of a direct  $T_{1/2} - N_{r,\odot}$  correlation, would – on the one hand – imply that **only**  ${}^{130}\text{Cd}$ ,  ${}^{131}\text{In}$  and the major part of  ${}^{129}\text{Ag}$  would be synthesized in  $\beta$ -flow equilibrium (see left side of Fig. 2); on the other hand, all  $N=82$  isotopes between  ${}^{124}\text{Mo}$  up to  ${}^{128}\text{Pd}$  would be produced in a steady flow, but not  ${}^{129}\text{Ag}$  to  ${}^{131}\text{In}$  (see right part of Fig. 2). At this point, I cannot refrain to point out, that this latter picture is the basis for the recent conclusions of Refs. [39,48]. These authors argue that *"the time spent at the  $N=82$  waiting point is shorter than previously assumed"* and *" ${}^{129}\text{Ag}$  and  ${}^{130}\text{Cd}$  cannot be produced in  $\beta$ -flow equilibrium"*. As demonstrated above, this conclusion is at least carried too far, if not wrong. Therefore, it is by all means unjustified to further conclude that their above result would imply *"that the  $N=82$  and  $N=126$  r-process peaks are made at two distinct sites"*. In any case, if the above authors were right, their conclusions would detract our contribution to the success in measuring r-process waiting-point nuclei, simply because other nuclear-physics quantities, such as neutron-capture cross sections, would substitute for the astrophysical significance of the  $\beta$ -decay properties in equilibrium scenarios.

In Fig. 3, we now present the results obtained with  $S_n$  values from the ETFSI-Q mass model, for the  $N=83$  isotones varying between 0.01 MeV for  ${}_{40}\text{Zr}$  via 1.09 MeV for  ${}_{44}\text{Ru}$  to 2.22 MeV for  ${}_{48}\text{Cd}$ . For further comparison, the left part shows the initial r-abundances of the waiting-point nuclei prior to  $\beta$ -decay back to stability; and in the right part the final r-abundances of the stable isobars after back-decay are depicted. It is evident already from the first glance, that with this approach the  $N_{r,\odot}$  pattern of the whole  $N=82$  waiting-point region between  $A=125$  and  $A=133$  is much better reproduced than under the simplified conditions leading to the two fits shown in Fig. 2. Since exactly the same  $\beta$ -decay quantities ( $T_{1/2}$  and  $P_n$ ) and astrophysics parameters (stellar temperature, neutron density, flow-time and weighting of the individual r-components) have been used,

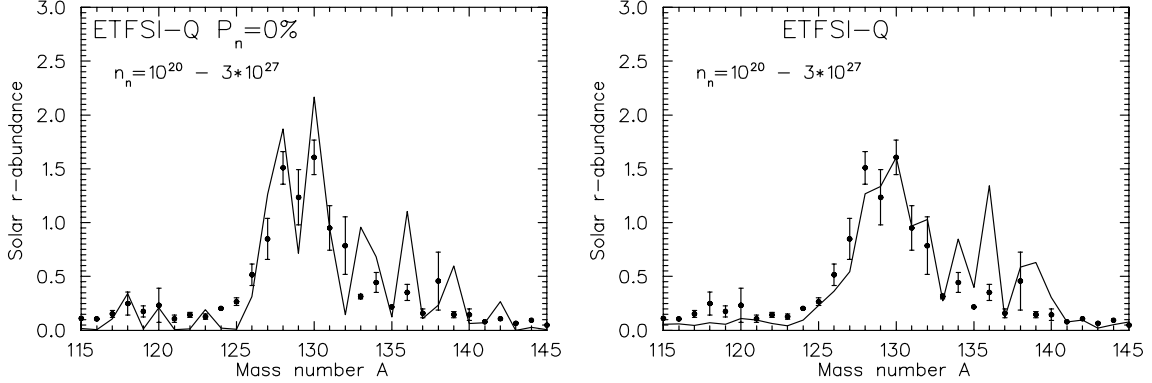


Figure 3. R-abundances in the  $A \simeq 130$  region from dynamical calculations with  $S_n$  values from the ETFSI-Q mass model. In the left part, the initial progenitor abundances are shown, prior to  $\beta$ -decay back to stability; in the right part, the final abundances of the stable isobars are depicted.

the improvements are clearly due to the increasing  $S_n$  values of the  $(N_{mag}+1)$  isotopes on the rising part of the  $A \simeq 130$  peak. Those  $N=82$  waiting-point isotopes at the bottom of the peak – with correspondingly ”low”  $S_n(N=83)$  values – collect r-abundance fractions for a much larger neutron-density range than the ones at the top of the peak with ”high”  $S_n(N=83)$  values. To be more specific, while in the  ${}_{46}\text{Pd}$  isotopic chain  $N=82$   ${}^{126}\text{Pd}$  is the major waiting-point nucleus up to  $n_n \simeq 10^{24} \text{ cm}^{-3}$ , the magic shell in the Ag chain is already passed at  $n_n \simeq 10^{23} \text{ cm}^{-3}$  and in the Cd chain even as early as  $n_n \simeq 10^{22} \text{ cm}^{-3}$ . Around  $n_n \simeq 10^{23} \text{ cm}^{-3}$ , the actual waiting-point in the Cd isotopic chain is 96 ms  $N=84$   ${}^{132}\text{Cd}$  [29]. Around  $n_n \simeq 10^{24} \text{ cm}^{-3}$ , even  $N=86$   ${}^{134}\text{Cd}$  takes over, and in the Ag chain  $N=84$   ${}^{131}\text{Ag}$  becomes the waiting-point nucleus. Hence, the final picture shown in the right part of Fig. 3 represents the sum of several (here altogether 16) partial equilibria, each for a definite neutron density, respectively r-process path. One may extend this discussion also to the regions below and beyond the actual abundance peak, where still some deficiencies exist. When focussing on the  $A=134$  to  $A=140$  area, which just has become within experimental reach [cite[klk:she]], the rather pronounced odd-even deviations seem to indicate an earlier onset of collectivity in very neutron-rich  ${}_{50}\text{Sn}$  to  ${}_{52}\text{Te}$  isotopes than commonly predicted. This would result in slightly higher  $S_n$  values in this region, thus shifting the r-process path further away from stability involving progenitor isotopes with shorter  $T_{1/2}$ .

Finally to the question, why to present the *initial progenitor abundances* in the left part of Fig. 3, which are no direct ”observables”? The reason is that in several recent papers discussing nucleosynthesis in the high-entropy bubble scenario of a SN II, charged-current neutrino reactions are predicted to significantly substitute for  $\beta$ -decays. This would require an extension from the classical  $\beta$ -flow equilibrium to a ”weak-flow” equilibrium (see, e.g. [49]). Also in this context, it was stated that a weak steady-flow equilibrium at  $N=82$  cannot be attained, which again would exclude  ${}^{129}\text{Ag}$  and  ${}^{130}\text{Cd}$  from this equilibrium. Qian et al. [50] argue that such neutrino-processing of the initial r-abundances during



freeze-out might help shorten the time-scale for the r-process and could be responsible for the "filling-up" of the low-mass wings of the  $A \simeq 130$  and  $A \simeq 195$   $N_{r,\odot}$  peaks. However, in this paper effects from  $\beta$ dn-emission during decay back to stability have been ignored completely. Based on our results shown in Fig. 3, where the left part corresponds to the "unprocessed distribution" of Fig. 2 in [50], we come to different conclusions. Already without considering additional abundance changes from capture of remaining seed neutrons and re-capture of delayed neutrons during freeze-out, we estimate that neutrino postprocessing effects are about an order of magnitude smaller than postulated by Qian et al. [50]. Our calculations suggest that the main effect of "filling-up" the initial under-abundances in the  $A=124-126$  region (see left part of Fig. 3) is due to  $\beta$ dn-branching during the first 150 ms of the freeze-out rather than neutrino-induced neutron spallation.

## 5. Summary

In this short review, I have tried to summarize our progress in studying nuclear properties of very neutron-rich isotopes that may be of importance in r-process nucleosynthesis. Although it has been a long and painstaking way over more than 15 years, there are still many open experimental and theoretical questions, among them also just the point discussed above about the astrophysical relevance of our data. If a careful evaluation of detailed network calculations would come to the conclusion that the nuclear-physics properties of the "classical"  $N=82$  waiting-point nuclei at the top of the  $A \simeq 130$  peak were, indeed, unimportant, we would accept it – most reluctantly. However, as long as this is not proven, we will endorse with Claus Rolf's recent affirmation at CGS-10: "*We will measure (it) anyhow...!*".

## Acknowledgements

I am very grateful to all my collaborators in the various nuclear-structure and astrophysics studies that formed the basis for this paper. In particular, I would like to thank Peter Möller and Friedel Thielemann for their patience in solving – or in terms of a nuclear-chemist *dissolving* – many problems. This work was supported by various grants from the German BMBF, DFG and FCI.

## REFERENCES

1. C.D. Coryell, J. Chem. Educ. 38 (1961) 67.
2. H.E. Suess and H.C. Urey, Rev. Mod. Phys. 28(1956) 53.
3. E.M. Burbidge et al., Rev. Mod. Phys. 29 (1957) 547.
4. E. Lund et al., Phys. Scr. 34 (1986) 614.
5. R.L. Gill et al., Phys. Rev. Lett. 56 (1986) 1874.
6. K.-L. Kratz et al., Z. Phys. A325 (1986) 489.
7. K.-L. Kratz, Rev. Mod. Astr. 1 (1988) 184.
8. P. Möller and J. Randrup, Nucl. Phys. A514 (1990) 1.
9. P. Möller et al., At. Data Nucl. Data Tables 59 (1995) 185.
10. K.-L. Kratz and F.-K. Thielemann, *Capture Gamma-Ray Spectroscopy and Related Topics*, World Scientific (1994) 724.

11. K.-L. Kratz et al., Ap. J. 403 (1993) 216.
12. F.-K. Thielemann et al., Nucl. Phys. A570 (1994) 329c.
13. K.-L. Kratz et al., Nucl. Phys. A630 (1998) 352c.
14. C. Freiburghaus et al., Ap. J. 516 (1999) 381.
15. K.-L. Kratz et al., Z. Phys. A340 (1991) 419.
16. K.-L. Kratz et al., Z. Phys. A336 (1990) 357.
17. K.-L. Kratz et al., Phys. Rev. C38 (1988) 278.
18. *Nuclear Structure of the Zr Region*, Res. Rep. in Phys., Springer (1988).
19. *Nuclei Far From Stability / Atomic Masses and Fundamental Constants 1992*, Inst. of Phys. Conf. Ser. **132** (1993).
20. *Exotic Nuclei and Atomic Masses - ENAM95*, Ed. Frontières (1995).
21. *Exotic Nuclei and Atomic Masses - ENAM98*, AIP Conf. Proc. 455 (1998).
22. *The ISOLDE Laboratory Portrait*, Hyperfine Interactions 129 (2000) 1.
23. B. Pfeiffer et al., Z. Phys. A357 (1997) 235.
24. *Fission and Properties of Neutron-Rich Nuclei*, World Scientific (1999).
25. *Fission and Properties of Fission-Product Nuclides*, AIP Conf. Proc. 447 (1998).
26. A. Korgul et al., Eur. Phys. J. A7 (2000) 167.
27. P. Hoff et al., Phys. Rev. Lett. 77 (1996) 1020.
28. N. Erdmann et al., Appl. Phys. B66 (1998) 431.
29. M. Hannawald et al., Phys. Rev. C62 (2000) 054301; and these proceedings.
30. Y. Aboussir et al., At. Data Nucl. Data Tables 61 (1995) 127.
31. G. Audi et al., Nucl. Phys. A624 (1997) 1.
32. T. Kautzsch et al., Eur. Phys. J. A9 (2000) 201.
33. J. Dobaczewski, The HFB/SkP Mass Table, priv. comm.
34. J.M. Pearson, The ETFSI-Q Mass Table, priv. comm.
35. B.A. Brown et al., priv. comm.; and to be published.
36. K.-L. Kratz et al., *Evaluation of  $T_{1/2}$  and  $P_n$  Values*, Kernchemie-Report, Mainz (1996), unpublished.
37. K. Takahashi et al., At. Data Nucl. Data Tables 12 (1973) 101.
38. P. Möller et al., At. Data Nucl. Data Tables 66 (1997) 131.
39. G. Martinez-Pinedo and K. Langanke, Phys. Rev. Lett. 83 (1999) 4502.
40. K.-L. Kratz et al., AIP Conf. Proc. 529 (1999) 295.
41. J. Shergur et al., Nucl. Phys. A, in print.
42. J.J. Cowan et al., Ap. J. 521 (1999) 194.
43. B. Pfeiffer et al., contribution to this conference.
44. J.W. Truran and J.J. Cowan, *Tenth Workshop on Nuclear Astrophysics*, MPI-Report (2000), in print.
45. S.E. Woosley et al., Ap. J. 433 (1994) 229.
46. K. Takahashi et al., Astron. Astrophys. 286 (1994) 857.
47. C. Arlandini et al., Ap. J. 525 (1999) 886.
48. K. Langanke and A. Poves, Nucl. Phys. News 10 (2000) 16.
49. G. McLaughlin and G.M. Fuller, Ap. J. 464 (1996) L143; and 489 (1997) 766.
50. Y.-Z. Qian et al., Ap. J. 494 (1998) 285.